

Crops Planting Information Retrieval at Farmland Plot Scale Using Multi-Sources Satellite Data

Huang Qiting^{1,2}, Luo Jiancheng¹, and Dong Wen¹

¹State Key Laboratory of Remote Sensing Science, Institute of Remote Sensing and Digital Earth, Chinese Academy of Sciences, Beijing, China

²University of Chinese Academy of Sciences, Beijing, China

Email: Huangqiting830112@163.com, Luojc@radi.cn

Abstract—With the development of precision agriculture and agricultural insurance, there are increasing demands for the fine-scale crops planting information in large areas. This paper presents a comprehensive approach for crop type identification and planting area estimation at a farmland plot scale by collaboratively utilizing the high-and-moderate spatial resolution satellite imagery. The proposed method roughly contains four steps: firstly, by implementing an image segmentation and a following manual editing, the objects of farmland plot with exact boundary are extracted from the high spatial resolution imagery; Secondly, with the effective-data processing technology and spectral indices calculation based on the multi-temporal moderate resolution images, the cloudlessly fragmentary effective data which served as the source of properties for plot objects is obtained; thirdly, the specific NDVI time-series and phenological parameters for each farmland plot are further derived from these effective data; Lastly, based on the multi-dimensional feature space of plot objects, the crop types and corresponding planting areas are mapped using the Random Forest Classifier. This approach has been tested for several crops in Sihong County, Jiangsu Province, China. The results showed that, this method can map the distribution of wheat, rice and corn at a farmland plot scale with relatively high accuracy. The user accuracy of wheat, rice and corn reached to 98.62%, 97.05% and 97.74%, respectively, and the overall accuracy was 95.36% with a Kappa coefficient of 0.936. The area accuracy of these three crops also amounted to 94.18%, 93.37% and 91.23%, respectively. This experiment illustrated the effectiveness and usefulness of the proposed method, and was referential to finely planting information extraction for other crops.

Index Terms—remote sensing, crop identification, farmland plot scale

I. INTRODUCTION

The application of remote sensing on crops planting information retrieval, such as crop types mapping, has long been studied. Since crops manifest differential spectral response in remotely sensed images at different stages of maturity, which enable building a crop-specific temporal record, most of these efforts make use of the low spatial resolution time-series data such as AVHRR or MODIS due to its high revisit frequency during crops

growing season [1]-[3]. There are also a considerable number of studies focusing on the crop type mapping using moderate (roughly 30m) resolution images with limitedly temporal coverage acquired at the critical time points in crop's lifecycle [4], [5]. Because of their low or moderate spatial resolution, they provide relatively coarse results and thus more suitable for large-scale investigation.

In order to obtain accurate crops planting information at a finer scale, several techniques have been developed in recent years [6], [7]. By merging the information from high-resolution low-time-frequency observation with low spatial resolution and high-temporal-frequency observations, Wu *et al.* [8] developed a spatial and temporal fusion approach to generate a new synthetic dataset with both high spatial and temporal resolution using the Landsat, GF1-WVF, HJ CCD and MODIS data. These synthetic dataset was then applied into the crops identification, and the results showed that the overall accuracy of crops classification reach 0.91 and 0.95 in the two test sites, respectively, both higher than those obtained by using multi-temporal Landsat data. Liu *et al.* [9] also proposed a synthetic data simulation method by minimizing the differences between the crop's ideal growing curve and that from the real observation, using different satellite data. The ideal curves of different crops were chosen from the pure pixel of time-series MODIS data and the real observations consisted of several medium resolution sensors. When applied into the crops identification, Liu concluded that up to 20% of improvement in classification accuracy can be achieved. There also exist many studies employing the object-oriented classification method, which based on an image segmentation, to conduct the crops investigation [10]-[12]. Generally, most of the studies adopt the high spatial resolution (0.2-5m) images from the satellite or aerial photography with only 1 or 2 temporal coverage during the crops' growing season. Although the multi-resolution fusion and the object-oriented methods can provide relative high classification accuracy at a finer scale, however, these high accuracy and spatial details may come at the cost of reduced temporal availability, highly financial expenditure and are often interfered with the presence of cloud. Therefore, they are to some extent not suitable for operational crops investigation at a finely field-scale, especially in areas where cloudy weather is common.

Manuscript received November 9, 2016; revised January 10, 2017.

With the development of precision agriculture and the increasing demands for higher investigation precision in agricultural management, agricultural insurance and disasters assessment, it is urgent to obtain the crops planting information at a farmland plot scale. The high spatial resolution satellite images is capable of delineating the precise outline of farmland plots, but limited in reflecting the growing features of crops due to its low temporal resolution; while the moderate spatial resolution images, with a relatively high temporal resolution, can recognize the growing properties although with a coarse spatial resolution. Therefore, it might be helpful to exploit the respective advances of both satellite data for achieving a better result.

This paper proposed a comprehensive approach for crops planting information retrieval at a farmland plot scale by combining the high and moderate resolution satellite data. The high resolution data adopted by this study was ZY-3 images, and the moderate data came from GF1-WVF sensors, which constituted a set of time-series images spanning the whole growing season at a time interval of roughly half a month. All the high and moderate images were geo-registered to the same reference image with a mean mis-registration error of no more than 1 pixel (16m). As a first step, the boundaries of farmland plots were extracted through implementing a multi-resolution segmentation on the high resolution image followed by a manual editing and smoothing. Secondly, with the effective-data processing technology and spectral indices calculation based on the multi-temporal moderate resolution imagery, the fragmentary effective data was acquired, and the time-series NDVI and derived phenological parameters for each object were further obtained from these effective data. Finally, the different crop types and corresponding planting areas were mapped using the Random Forest Classifier.

This approach has been tested for several crops in Sihong County, Jiangsu Province, China. The results showed that, this method can map the crop types and corresponding planting areas at a level of farmland plot with relatively high accuracy. The user accuracy of wheat, rice and corn reached to 98.62%, 97.05% and 97.74%, respectively, and the overall accuracy was 95.36% with a Kappa coefficient of 0.936. When compared with the published statistic data of crops planting area, the area accuracy of these three crops also amounted to 94.18%, 93.37% and 91.23%, respectively. This study illustrated the effectiveness and usefulness of the proposed method, and also provided a salutary lesson for finely planting information extraction for other crops.

II. METHODOLOGY

The proposed method takes the high resolution images as the source of “detailed structure information” such as farmland plot boundary, and regards the time-series moderate resolution images as the raw materials for “properties information” like spectral and phenological features. By fusing the “properties information” with the farmland plot object, the crop type and planting area can be retrieved for each plot through the implementation of crop classification model. Furthermore, in order to avoid the influences of cloud cover and cloud shadow, and to increase the data coverage in areas where rainy and/or cloudy weather is commonly appeared during the growth season of crops, a data processing method called Effective Data Processing Technology is applied into the multi-temporal moderate resolution images. As showed in Fig. 1, the proposed method mainly consists of four components: (a) farmland plot extraction; (b) Effective-data processing of multi-temporal moderate images; (c) acquisition of farmland plot properties; (d) crops identification. Each of these components will be detailed in the following sections.

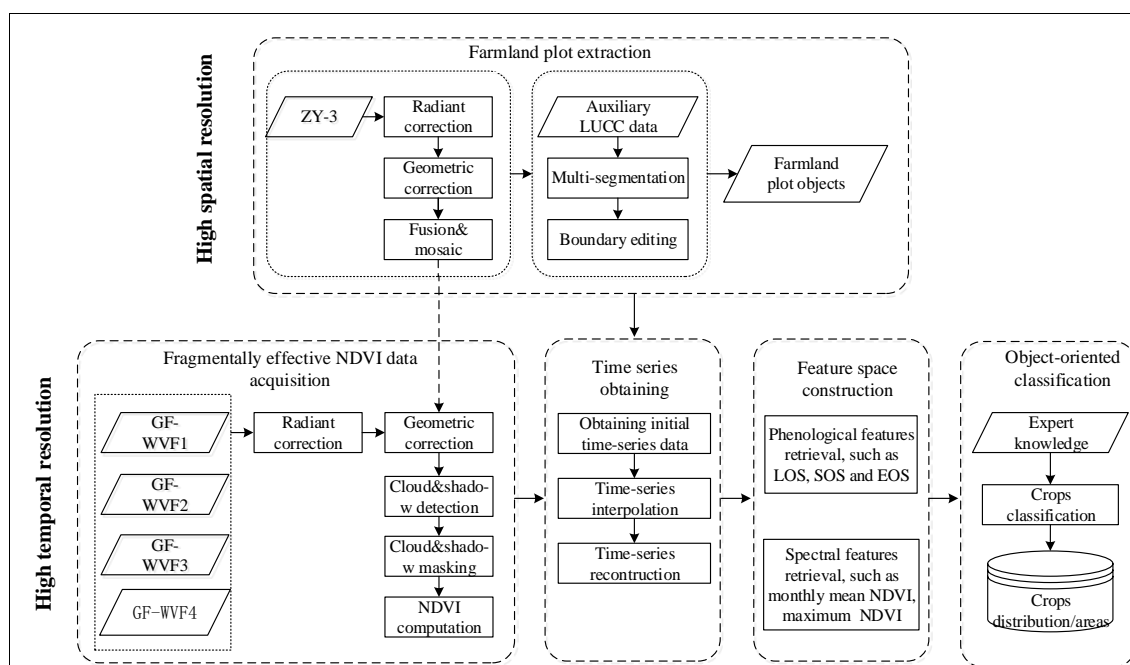


Figure 1. The flowchart of the proposed method

A. Farmland Plot Extraction

With appropriate resolution of 2m, the ZY-3 fusion image is not only capable of discerning the detailed structure of plots (e.g., farmland plot boundaries) but also can minimize the inner spectral heterogeneity, which is therefore suitable for farmland plot extraction through image segmentation. In this paper, we first located the distribution of farmland areas with the help of auxiliary LUCC(Land Use and Land Cover Change, LUCC) data, then applied a multi-resolution segmentation on these regions and the preliminary objects of farmland plot were obtained. Finally, to enhance the positioning accuracy of the plots, these objects with jagged boundaries were manually edited and smoothed (see Fig. 2). Although the extraction of farmland plot needs quite a few manual editing, it has relatively high reusability and is beneficial to the latter fast update considering the temporal stability of farmland plot boundaries.



Figure 2. The farmland plot extraction result

B. Effective-Data Processing of Multi-Temporal Moderate Images

When cloud cover exceeded certain percent (e.g., 70%), an image is often regarded as useless data and is abandoned in traditional remote sensing application, which may cause the problem of data missing in spatial or temporal coverage. This method, by contrast, takes those heavy cloud-cover images as also an important source of information by using the effective-data processing technology based on cloud and cloud-shadow detection. It extracts the non-cloud pixels from the gaps between cloud-cover regions and use these “useful pixels” in a form of cloudlessly fragmentary “data pieces”, thus significantly increasing the spatio-temporal coverage of remote sensing data. As mentioned above, the cloud and cloud-shadow detection plays a key role in the effective-data processing. Here we adopt the cloud detection method proposed by Zhou [13], which first transforms images into the $YCbCr$ space from original RGB to enhance the contrast of cloud and shadow with background pixels, then employs an Otsu algorithm to automatically determine the threshold values for cloud and shadow respectively. By segmenting the enhanced image with these thresh values, the distribution of cloud and shadow are finally detected (for more details, one can

refer to [13]). After that, the fragmentary effective-data can be obtained by masking images with the corresponding results of cloud and shadow detection, and the NDVI dataset will be further calculated based on these effective data. Fig. 3 demonstrates the processing chain of effective-data and NDVI dataset.

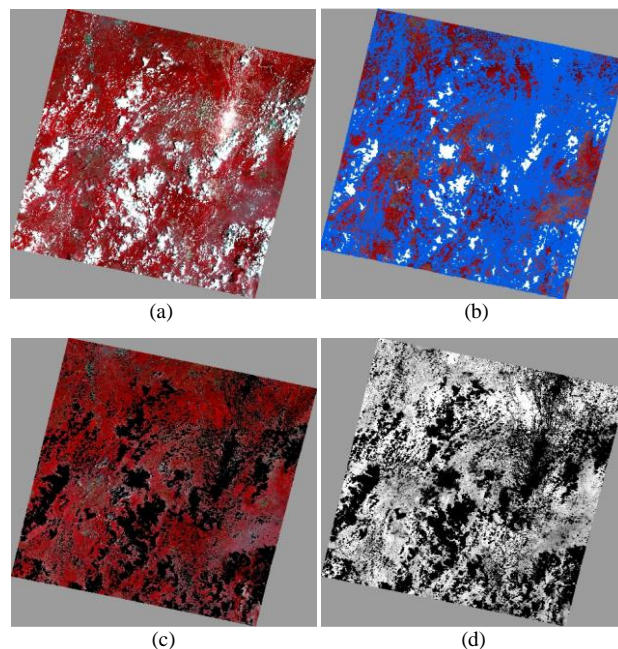


Figure 3. Demonstration of effective data processing: (a) raw image; (b) results of cloud detection; (c) cloud and shadow removal; (d) fragmentary NDVI data

C. Acquisition of Farmland Plot Properties

1) Normalization of different sensors' NDVI

Since the time-series NDVI dataset consisted of several satellite sensors, there may exist variations in the NDVI values due to the differences between sensors such as band width, spectral respond function or observation geometry, which in turn will bring uncertainties in subsequent application. Generally, these variations can be viewed as systematic deviation, and therefore can be calibrated with a linear regression fitting. In this paper, the GF-WVF1 was chosen as standard sensor, and the NDVI from other sensor, which covering the same areas in the same date as GF-WVF1, was acquired to build the regression model. For more information about the linear inter-sensors' NDVI calibration, one can refer to the reference [14]. Table I shows the resultant calibration models between GF-WVF1 and other sensors. With these regression models, the normalization of raw NDVI dataset was accomplished.

TABLE I. REGRESSION MODELS OF GF-WVF1 AGAINST OTHER SENSORS

Sensor	Fitting equation	R ²	RMSE
GF1-WVF2	$Y=0.769X+0.1699$	0.8977	0.0195
GF1-WVF3	$Y=0.8233X+0.1285$	0.6362	0.0416
GF1-WVF4	$Y=0.9195X+0.0446$	0.7975	0.0339

* Y: NDVI of GF-WVF1; X: NDVI of other sensors

2) Time-series acquisition and reconstruction

Based on the calibrated NDVI dataset, preliminary time series of NDVI for farmland plots were obtained by taking each plot as a basic unit. However, the temporally observation distribution of individual plot may largely differ because of the use of fragmentary effective-data. This heterogeneously temporal coverage of farmland plots makes the design and training of classifiers much more complex and may introduce artifacts, both in terms of continuity, but also in terms of classification accuracy. To solve these problem, Inglada *et al.* [6] use a linear interpolation to resample the time-series images on the same temporal grid. Similarly, we first interpolated all the time series using the SPLINE function with a fixed time interval, then further reconstructed by the Savitzky-Golay filter, see Fig. 4.

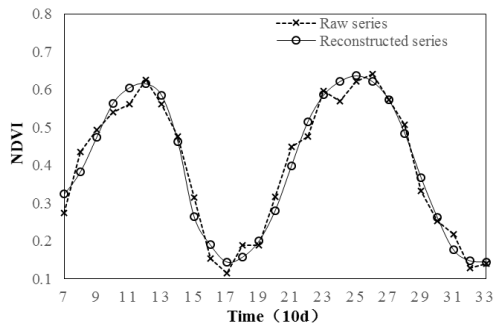


Figure 4. The contrast of NDVI time-series reconstruction

3) Extraction of farmland plot properties

Crops present specific spectral features at different growth stages, which can be reflected in the changes of NDVI time series. In other words, the NDVI time-series curves is capable of depicting the phenological characteristics of crops, and thereby possesses potential for distinguishing crop types with their specific phenology.

TABLE II. THE PHONOLOGICAL AND SPECTRAL PROPERTIES USED IN THIS STUDY

Property	Meaning	Property	Meaning
SOS	Start of growing season, the time when NDVI become higher than 20% of maximum value.	EVI	Enhanced vegetation index.
EOS	End of growing season, the time when NDVI become lower than 20% of maximum value.	NDWI	Normalized difference water index
LOS	Long of growing season, the time period between SOS and EOS.	NIR	Near Infrared band value
MOS	Maximum NDVI of growing season.	Maximum of NIR	Maximum NIR band value of growing season
WR	Withering rate, the rate from MOS to EOF.	Minimum of NDVI	Minimum NDVI of growing season
NDVI	Normalized difference vegetation index.	Minimum of NIR	Minimum NIR band value of growing season
RVI	Ratio vegetation index.		

* The spectral properties such as NDVI are statistically calculated for each month.

By far many studies have been carried out for vegetation phenology monitoring or crops planting

information extraction using remote sensing data. Although most of these studies focused on the low resolution time-series images, the developed approaches and relevant phenological parameters are still beneficial to our study. In this paper, both of the spectral and phenological properties were utilized to construct a feature space for crops identification. The phenological parameters were calculated with a dynamic threshold method [15] and consisted of 1) maximum value in NDVI series, MOS; 2) start of growing season, SOS; 3) end of growing season, EOS; 4) long of growing season, LOS; 5) withering rate, WR. The spectral properties included a variety of vegetation indices and band values represented in various statistically forms. Parts of these properties were listed in Table II. Fig. 5 shows the geometrical meaning of these phenological parameters.

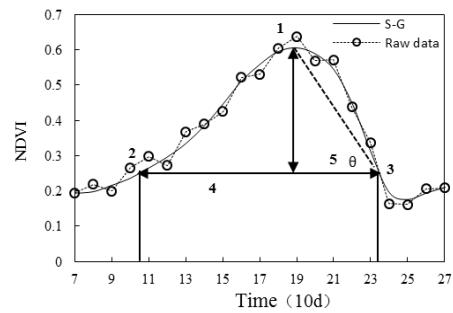


Figure 5. Remote sensing phenological features derived from NDVI curve

D. Crops Identification

The Random Forest (RF) algorithm was developed by Breiman [16] and recently has become one of the most popular Ensemble Learning technologies. It consists of an arbitrary number of simple trees, which are used to determine the final outcome. For classification problems, the ensemble of simple trees vote for the most popular class. This algorithm has been approved to be capable of handling a large number of variables without variable selection, and running efficiently on large dataset. Meanwhile, it can provide estimates of what variables are important in the classification. Considering the variables volume and their complicated relationship in the feature space, we employed the random forest algorithm as the classifier in this study.

III. EXPERIMENT AND RESULTS

A. Study Areas

The presented method was tested in Sihong county, Which is located between 117°56'E-118°46'E and 33°08'N-33°44'N in the northwest of the Jiangsu province, see Fig. 6. This areas is strongly influenced by the East Asian monsoon and the topography is characterized by the plain and downland with sparing hills distributed in the southeast. Because of the monsoon and its location near the Hongze Lake, the cloudy/rainy weather is common in this region, especially in summer. The wheat, rice and corn constitute the three main crops in this area, and besides that, the soybean, peanut and

watermelon are also commonly planted. the cropping system mainly includes two types, i.e., wheat-single season rice and wheat-corn.

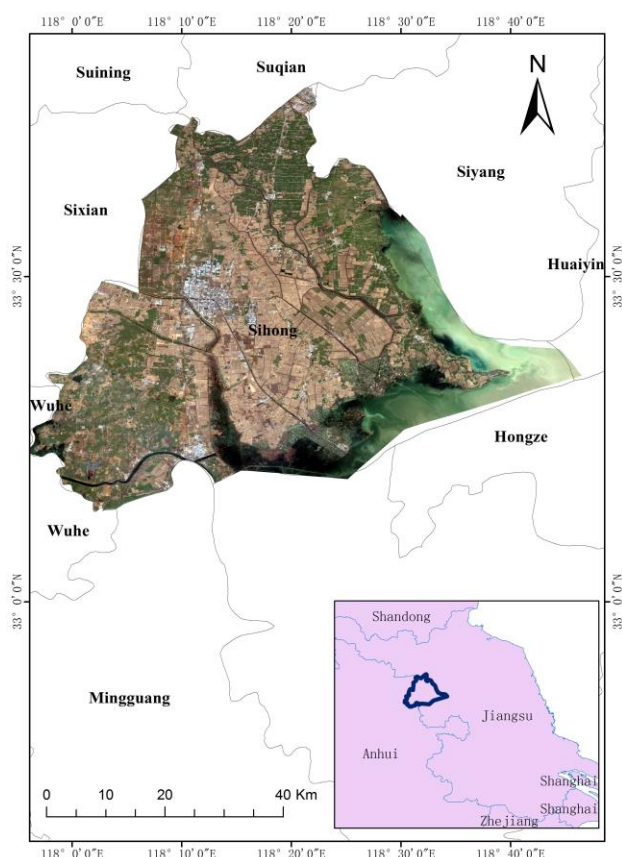


Figure 6. The location of study area

B. Data Sources and Preprocessing

Both satellite data and land cover map were used in this study. The cloudless 2m ZY-3 data was adopted as high resolution image and, the moderate data consisted of images from GF1-WFV sensors and constituted a time-series dataset spanning from March 2015 to November 2015 at a time interval of approximate 15 days. More information about the data sources was listed in Table III.

TABLE III. THE SATELLITE DATA USED IN THIS STUDY

Date	Location	Sensor	Date	Location	Sensor
20150312	E117.9N32.6	WFV2	20150823	E117.9N34.2	WFV2
20150312	E118.3N34.2	WFV2	20150901	E117.9N33.4	WFV4
20150328	E118.3N32.9	WFV1	20150828	E117.1N33.4	WFV4
20150414	E119.0N33.9	WFV3	20150908	E118.1N32.9	WFV1
20150422	E118.0N32.6	WFV2	20150921	E119.1N33.9	WFV3
20150422	E118.4N34.2	WFV2	20150925	E118.4N34.3	WFV2
20150501	E117.2N33.4	WFV4	20151003	E119.2N34.2	WFV2
20150516	E119.3N32.9	WFV1	20151012	E117.6N33.4	WFV4
20150525	E119.0N33.9	WFV3	20151015	E119.2N32.9	WFV1
20150606	E118.5N32.6	WFV2	20151020	E118.5N33.5	WFV4
20150606	E118.9N34.2	WFV2	20151027	E119.1N32.9	WFV1
20150619	E117.2N33.5	WFV4	20151102	E116.4N33.3	WFV4
20150705	E116.7N32.6	WFV2	20151114	E116.6N33.4	WFV4
20150713	E117.9N33.6	WFV2	20151129	E119.2N32.9	WFV1
20150713	E118.3N34.2	WFV2	20130321	E118.4N33.4	ZY3
20150725	E117.8N32.9	WFV1	20130321	E118.3N33.1	ZY3
20150730	E119.2N33.4	WFV4	20130311	E117.8N33.4	ZY3
20150803	E119.1N33.5	WFV4	20130311	E117.7N33.1	ZY3
20150823	E117.5N32.6	WFV2			

All the high and moderate images were first radiometrically corrected to obtain the surface reflectance using 6S model, and then geo-registered to the same reference image with a mean mis-registration error of no more than 1 pixel (16m). After that, these new dataset was served as input into the proposed method for crops identification and planting areas estimation.

C. Crops Growing Characters and Crops Classification

As showed in Fig. 7, there exist obvious differences in the shape and magnitude between different NDVI curves, which reflect the specific growing patterns of different crop types. These temporal discrepancy of NDVI changes forms the basis for phenology analysis, and is helpful to crops classification by enlarging the separability of different crop types which may present similar spectral features in certain time point. For example, the spectral features of peanut and rice may look alike in the late July (about at the point of 21st in time-axis), however, they can be temporally differentiated with the differences in their specific SOS (start of growing season) and LOS (long of growing season).

In this study, the crop types were distinguished into wheat, rice and corn, and all other farmland vegetation (including other crops and non-crop plants) were together labeled as “others”. In order to acquire the ground truth data, two field survey were carried out in June 2015 and October 2015. By using the GPS positioning technology, we obtained a total number of 520 plot samples for the three main crops, and 84 plots for others. These samples were randomly grouped into two parts, i.e., the modeling and validation samples. In the end, a random forest classifier with 1000 trees was employed and trained based on the modeling samples and then applied into the rest of farmland plots.

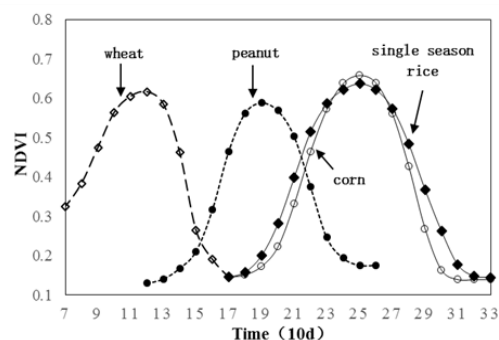


Figure 7. Reconstructed NDVI curves of crops belonging to different crop-rotation composition

D. Results and Accuracy Evaluation

The distribution of wheat was showed in Fig. 8a. It predominated in the study areas and represented as the most widely planted crop in the first half of the year. The distribution of rice and corn were showed in Fig. 9a. It can be seen that there existed different patterns in their spatial distribution. The rice was concentrated in the south and central parts of the study area where the plain is the predominant topography and irrigation facilities are conveniently available. Meanwhile, in the downland areas

lacking of enough irrigation system, surrounding the rice planting regions, the corn was mainly grew. As showed in Fig. 8b and Fig. 9b, these crops were mapped at a

farmland plot scale, which is beneficial to ground-based verification and further precise application.

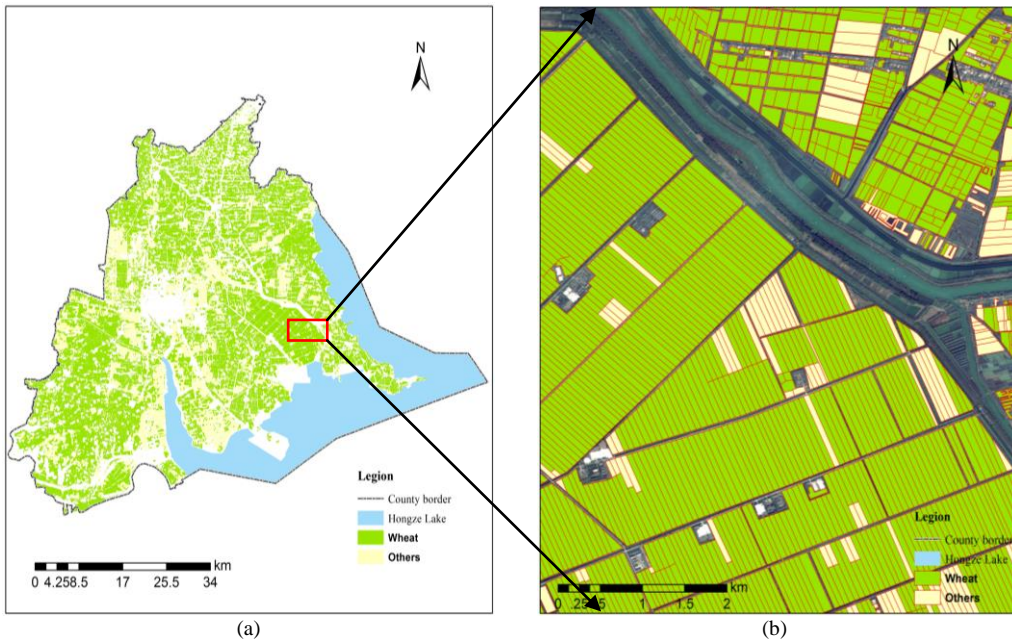


Figure 8. Distribution of wheat at farmland plot scale

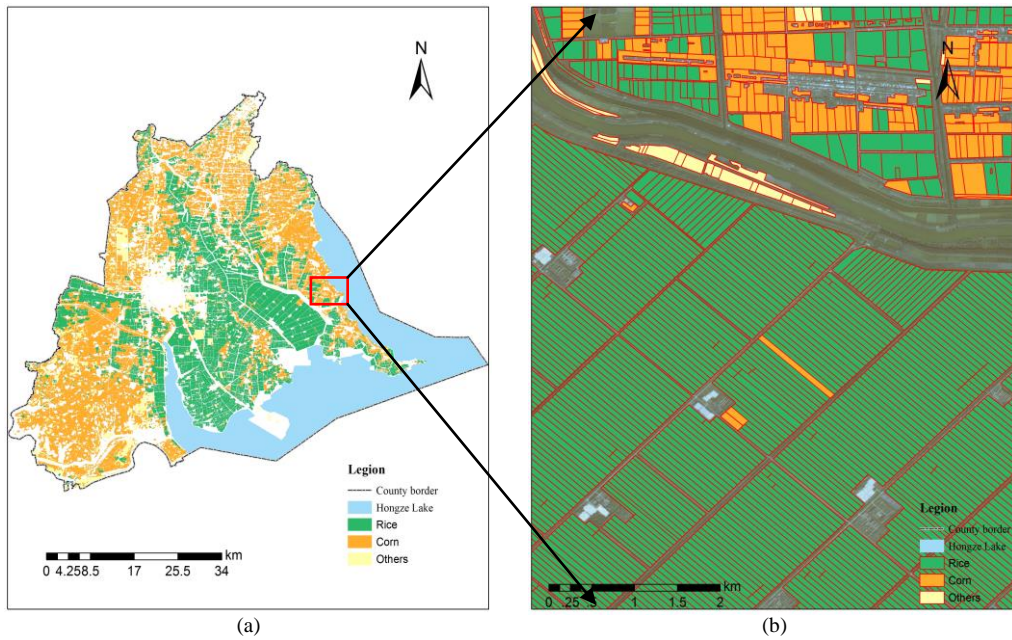


Figure 9. Distribution of rice and corn at farmland plot scale

The confusion matrix was listed in Table IV. The user accuracy of the crops, i.e., wheat, rice and corn, reached to 98.62%, 97.05% and 97.74%, respectively, and the overall accuracy was 95.36% with a Kappa coefficient of 0.936. Table V was the corresponding planting areas of these crops. When compared with published statistical data, the derived area accuracy of these three crops also amounted to 94.18%, 93.37% and 91.23%, respectively. Both of classification and area estimation can achieved a satisfactory accuracy in this study, and demonstrated the effectiveness of the proposed method.

TABLE IV. CONFUSION MATRIX FOR CROPS CLASSIFICATION

Crop types	Wheat	Rice	Corn	Others	Total	User Accuracy (%)
Wheat	214	0	0	3	217	98.62
Rice	0	156	0	4	160	97.05
Corn	0	2	130	1	133	97.74
Others	5	5	8	76	94	80.85
Total	219	163	138	84	604	
Mapping accuracy(%)		97.72	95.71	90.47		
Overall accuracy(%)		95.36				
Kappa		0.936				

TABLE V. AREA ACCURACY OF CROPS PLANTING AREA EXTRACTION

Crop types	Retrieved area (1,000ha)	Published area (1,000ha)	Area accuracy (%)
Wheat	97.32	103.33	94.18
Rice	55.37	59.30	93.37
Corn	38.15	41.82	91.23
Total area	190.84	204.45	
Mean	—	—	93.34

IV. CONCLUSION AND DISCUSSION

This paper presented a method of crops identification and planting areas estimation at farmland plot scale based on the combination of high and moderate resolution satellite data. By taking the Sihong county in Jiangsu province as study area, the proposed method was tested on the wheat, rice and corn classification and corresponding planting areas estimation. The results showed that this method possess promising potential for crop planting information retrieval with the overall accuracy of classification and planting areas estimation reaching 95.36% and 93.34%, respectively. It is also safe to draw some conclusions as follows:

a) Taking farmland plot as the basic unit in classification can prevent the ‘peper’ phenomenon which often encountered with traditional image classification, thus increasing the accuracy and variability of classified results.

b) The combination of multi-sources images and the use of effective-data technology can significantly increase the spatio-temporal coverage of data, therefore providing strong support for crops monitoring especially in regions where rainy/cloudy weather commonly appeared.

c) By collaboratively utilizing the information derived from both the high and moderate resolution satellite data and, by introducing phonological characters into the classification, this method can effectively enhance the separability of crops at a fine scale, thereby increasing the accuracy of crops identification in both space and properties. Although our method can achieve generally satisfactory performance, there are some aspects still to be improved. One is the acquisition of farmland plots which by far still needs quite a few manual editing. More efforts should be put into the optimization of image segmentation algorithm, to get more spatially accurate boundaries of farmland plot and reach a higher level of automation. Another aspect is dealing with the high degree of fragmentation and heterogeneity of farmland plots. In that case, the size of farmland plot is often smaller than that of pixels, therefore the spectral unmixing approaches should be introduced to solve this problem.

ACKNOWLEDGMENT

The authors thank China Centre for Resources Satellite Data and Application for providing the satellite data. This work was supported by Natural Science Foundation of China (41301473; 41301438), the National High Technology Research and Development Program of China (2015AA123901) and the Science and Technology Project of Guangxi Province (14125008-1-6).

REFERENCES

- [1] M. J. Hill and G. E. Donald, “Estimating spatio-temporal patterns of agricultural productivity in fragmented landscapes using AVHRR NDVI time series,” *Remote Sens. Environ.*, vol. 84, no. 3, pp. 367-384, Mar. 2003.
- [2] B. D. Wardlow, S. L. Egbert, and J. H. Kastens, “Analysis of time-series MODIS 250m vegetation index data for crop classification in the U.S. central Great Plains,” *Remote Sens. Environ.*, vol. 108, no. 3, pp. 290-310, Jun. 2007.
- [3] M. Ozdogan, “The spatial distribution of crop types from MODIS data: Temporal unmixing using independent component analysis,” *Remote Sens. Environ.*, vol. 114, no. 6, pp. 1190-1204, Jun. 2010.
- [4] H. X. Zhang, *et al.*, “Research on crop identification using multi-temporal NDVI HJ images,” *Remot. Sens. Techno. Appl.*, vol. 30, no. 2, pp. 304-311, Apr. 2015.
- [5] K. Jia, B. F. Wu, and Q. Z. Li, “Crop classification using HJ satellite multispectral data in the North China Plain,” *J. Appl. Remote Sens.*, vol. 7, no. 8, pp. 287-297, Jan. 2013.
- [6] J. Inglada, *et al.*, “Assessment of an operational system for crop type map production using high temporal and spatial resolution satellite optical imagery,” *Remote Sens.*, vol. 7, pp. 12356-12379, Sep. 2015.
- [7] S. Valero, *et al.*, “Production of a dynamic cropland mask by processing remote sensing image series at high temporal and spatial resolutions,” *Remot. Sens.*, vol. 8, pp. 10055-10076, Jan. 2016.
- [8] M. Q. Wu, *et al.*, “Reconstruction of daily 30m data from HJ CCD, GF-1 WFV, LANDSAT, and MODIS data for crop monitoring,” *Remot. Sens.*, vol. 7, pp. 16293-16314, Dec. 2015.
- [9] W. M. Liu, M. Ozdogan, and X. J. Zhu, “Crop type classification by simultaneous use of satellite images of different resolutions,” *IEEE Trans. Geosci. Remote Sens.*, vol. 52, no. 6, pp. 3637-3649, Jun. 2014.
- [10] J. Peřa, P. Guti erez, and C. Herv ́asmart ́nez, “Object-Based image classification of summer crops with machine learning methods,” *Remote Sens.*, vol. 6, no. 6, pp. 5019-5041, May 2014..
- [11] Q. Yu, *et al.*, “Object-based detailed vegetation classification with airborne high spatial resolution remote sensing imagery,” *Photogramm. Eng. Rem. S.*, vol. 72, no. 7, pp. 799-811, July 2006.
- [12] C. D. Dennis, *et al.*, “A comparison of pixel-based and object-based image analysis with selected machine learning algorithms for the classification of agricultural landscapes using SPOT-5 HRG imagery,” *Remote Sens. Environ.*, vol. 118, no. 15, pp. 259-272, Mar. 2012.
- [13] W. Zhou, *et al.*, “Automatic detection and repairing of cloud and shadow regions in multi-spectral remote sensing images,” *J. Remot. Sens.*, vol. 16, no. 1, pp. 132-142, Jan. 2012.
- [14] M. D. Steven, *et al.*, “Inter-calibration of vegetation indices from different sensor systems,” *Remote Sens. Environ.*, vol. 88, no. 4, pp. 412-422, Dec. 2003.
- [15] Z. Li, *et al.*, “LULC classification based on random forest with aid of phonological features,” *Remot. Sens. Inf.*, vol. 28, no. 6, pp. 48-55, June 2013.
- [16] L. Breiman, “Random forest,” *Machine Learning*, vol. 45, no. 1, pp. 5-32, Jan. 2001.



Qiting Huang was born in China in 1983. He received the B.S. degree in Agricultural resources and environments from the Hunan Agricultural University, Changsha, Hunan, China, in 2006 and the M.S. degree in Agricultural remote sensing and information technology from Zhejiang University, Hangzhou, Zhejiang province, China. He is now a Ph.D. candidate in University of Chinese Academy of Sciences. His research interests include remote sensing of crops and crop yields, precision agriculture, land-use changes and remote sensing data processing.



Jiancheng Luo received the B.S. degree in computer science from Zhejiang University, Hangzhou, Zhejiang province, China and M.S. and Ph.D. degree in cartography and geographical information system from the institute of geographic sciences and natural resources research, Chinese Academy of Sciences, in Beijing, China. His research interests include remote sensing information extraction, land-use changes and data mining.



Wen Dong received the B.S. degree in computer science from China Agriculture University, Beijing, China and M.S. and Ph.D. degree in cartography and geographical information system from the institute of remote sensing and digital earth, Chinese Academy of Sciences, in Beijing, China. Her research interests include remote sensing information extraction, database engineering and data mining.